Insect Biochemistry and Molecular Biology 112 (2019) 103206

Contents lists available at ScienceDirect

Insect Biochemistry and Molecular Biology

journal homepage: www.elsevier.com/locate/ibmb

The wing-specific cuticular protein LmACP7 is essential for normal wing morphogenesis in the migratory locust

Xiaoming Zhao[a,1], Xin Gou[a,b,1], Weimin Liu[a], Enbo Ma[a], Bernard Moussian[c], Sheng Li[d], KunYan Zhu[e], Jianzhen Zhang[a,*]

[a] Institute of Applied Biology, Shanxi University, Taiyuan, Shanxi, 030006, China
[b] College of Life Science, Shanxi University, Taiyuan, Shanxi, 030006, China
[c] Université Côte d'Azur, CNRS, Inserm, Institute of Biology Valrose, Parc Valrose, 06108, Nice CEDEX 2, France
[d] Guangzhou Key Laboratory of Insect Development Regulation and Application Research, Institute of Insect Sciences and School of Life Sciences, South China Normal University, Guangzhou, 510631, China
[e] Department of Entomology, 123 Waters Hall, Kansas State University, Manhattan, KS, 66506, USA

ARTICLE INFO

Keywords:
Wing development
LmACP7
Endocuticle
Epithelial cell
Apoptosis-like
Locusta migratoria

ABSTRACT

Wings are an indispensable structure in many insects for their foraging, courtship, escape from predators, and migration. Cuticular proteins are major components of the insect cuticle and wings, but there is limited information on how cuticular proteins may play an essential role in wing morphogenesis. We identified a wing-specific cuticular protein, LmACP7, which belongs to the RR-2 subfamily of CPR chitin-binding proteins in the migratory locust. LmACP7 was initially produced in epidermal cells and subsequently migrated to the exocuticle at the pre-ecdysial stage in adult wings. Depletion of *LmACP7* transcripts by RNA interference markedly reduced its protein amounts, which consequently led to abnormal wing morphogenesis. The deformed wings were curved, wrinkled, and failed to fully expand. We further demonstrated that the deformation was caused by both severe damage of the endocuticle and death of the epidermal cells in the wings. Based on these data, we propose that LmACP7 not only serves as an essential structural protein in the wing but is also required for the integrity of wing epithelial cells. LmACP7 contributes to production of the wing endocuticle and to the morphogenesis of functional wings in the migratory locust.

1. Introduction

Among invertebrates, insects are the only taxon that have the ability to fly. Their wings evolved around 350 million years ago. Insect wings are derived from the ectoderm, and play important roles in foraging, courtship, protection against predators, and migratory flight. They consist of a thin membrane stabilized by a reticulate system of veins and are functional only in the adult insect. Within each of the major veins there is a nerve and a respiratory tube, a trachea. Since the lumens of the veins are connected with the hemocoel, veins are filled with hemolymph (Simpson and Douglas, 2013). Unlike bird wings, wings of holometabolous insect species develop internally as larval organs in the body of insects such as butterflies and beetles, whereas the wings are formed from the wing pads of the nymph in hemimetabolous insects such as locusts (Klowden, 2008). Wings (wing pads) are composed of two layers of epidermal cells that secrete and organize the dorsal (upper) and ventral (lower) cuticular layers (Chen et al., 2007). As the wing matures, the epidermal layers are reduced in size, possibly dying or fusing together. In the developing protective forewing (elytron) of the red flour beetle (*Tribolium castaneum*), the space between these two layers is filled with hemolymph and structures known as trabeculae that function as mechanical struts, connect and fortify the dorsal and ventral cuticular layers (Arakane et al., 2012; Noh et al., 2017).

The cuticle that shapes the wing is divided into the epicuticle, exocuticle and endocuticle from outside to inside (Appel et al., 2015; Rajabi et al., 2016). In the wing veins of dragonflies and the rigid elytral cuticle of *T. castaneum*, the cuticular layers have a unique ultrastructural architecture which is composed of the envelope, epicuticle, exocuticle and endocuticle as revealed by scanning electron microscopic (SEM) and transmission electron microscopic (TEM) analyses (Appel et al., 2015; Noh et al., 2016). The envelope, epi- and exocuticle are secreted prior to ecdysis and the endocuticle is generally formed

* Corresponding author.
E-mail address: zjz@sxu.edu.cn (J. Zhang).
[1] These authors contributed equally to this work.

https://doi.org/10.1016/j.ibmb.2019.103206
Received 25 March 2019; Received in revised form 10 July 2019; Accepted 15 July 2019
Available online 16 August 2019
0965-1748/

after ecdysis (Moussian, 2010; Noh et al., 2017). Like epidermal cells, the wing epithelial cells are also involved in the formation of a basal extracellular matrix.

Wing morphology is not only defined by the cuticle, but also by the underlying epithelial cells. The formation of cell junctions is a crucial step during epithelial development as it ensures correct organization and function of the entire tissue (Bloor and Kiehart, 2002). Wing epithelial cells are held together by several types of junctional contacts below the subapical region, which not only mediate adhesiveness (adherens junctions, AJ) but also prevent the passage of small molecules (septate junctions, SJ) and facilitate cellular communication (gap junctions, GJ). Extending from the epidermis to the inner epicuticle there are so-called pore canals that with a diameter of 1 μm or less are involved in material transport to the surface.

Cuticular proteins (CPs) and the polysaccharide chitin are the primary structural components of the exo- and endocuticle layers that comprise the procuticle. In the process of molting, CPs are periodically synthesized (Charles, 2010). CPs expressed before ecdysis are called pre-ecdysial proteins, whereas those expressed after ecdysis are called post-ecdysial proteins. Insect CPs are classified into several distinct families defined by the presence of specific sequence motifs (Togawa et al., 2007; Willis, 2010). The largest of these is the CPR family, which includes proteins that have a conserved amino acid sequence known as the Rebers & Riddiford (R&R) motif (Rebers and Riddiford, 1988). The R&R motif is a chitin-binding domain that may mediate the interaction between chitin fibers and the proteinaceous matrix (Rebers and Willis, 2001; Togawa et al., 2004). Expression of specific CPs are possibly required to produce cuticles with a wide range of morphological and mechanical properties in different regions of the insect body and at different developmental stages (Cornman et al., 2008; Dittmer et al., 2012; Futahashi et al., 2008; Karouzou et al., 2007; Roer et al., 2015). In theory, the degree of cross-linking of some CPs together with cuticle dehydration are critical for determining appropriate mechanical properties such as rigidity or flexibility (Noh et al., 2016). In *T. castaneum*, analyses of TcCPR27, TcCPR18, TcCPR4 and TcCP30 which are the most abundant wing cuticular proteins, have provided insights into the roles of CPs in organizing the cuticle and determining its properties (Arakane et al., 2012; Mun et al., 2015; Noh et al., 2014, 2015). However, further investigation is needed to identify CP(s) specifically involved in the formation and function of the cuticle of a flyable insect wing and to characterize the precise timing of their appearance and location, their transport into and throughout the cuticle.

The migratory locust (*Locusta migratoria*) is one of the most destructive agricultural pests, which has powerful fore- and hindwings for long-distance migration. In a previous study, several proteins were purified from the wing cuticle of pharate adult locusts and their amino acid sequences were determined by combined use of mass spectrometry and automated Edman degradation (Krogh et al., 1995). We identified and confirmed the sequences of the respective open reading frames in the transcriptome of *L. migratoria* (Zhao et al., 2017). Among these genes, we identified *LmACP7* that codes for a CPR family protein with a RR-2 motif. In the present study, we revealed the developmental stage- and tissue-dependent expression profiles of *LmACP7*, determined the localization of its encoded protein in the wing pads from the fifth-instar nymphs to adults by immunohistochemistry, and precisely localized the protein within the adult wing by TEM and immunogold labeling. RNAi was utilized to investigate its roles in the formation of the adult wing cuticle. Our results indicate that LmACP7 is required for normal wing morphogenesis as an essential structural component in the wing cuticle.

2. Methods and materials

2.1. Insects

Eggs of *L. migratoria* were incubated at 30 ± 1 °C, 50% relative humidity, and with a 14-h-light/10-h-dark photoperiod in the laboratory. After 10 days, the nymphs were reared on fresh wheat sprouts under the same conditions (Guo et al., 2012). The wheat bran was supplemented after the nymphs reached the fifth instar stage and these nymphs were used for RNAi, isolation of total RNA and proteins in this study.

2.2. Identification and bioinformatic analysis of LmACP7

The cDNA sequences of the target genes were searched from the transcriptomic data from the dissected nymphal wing discs (GBDZ00000000) and the genome of *L. migratoria* (AVCP: *Locusta migratoria*, whole genome shotgun sequencing project). Conceptual translation of cDNA sequences was carried out with translation tools at ExPASy (http://www.expasy.org/tools/dna.html). The deduced protein domains were determined by SMART (http://smart.embl.de/). Analyses of deduced amino acid sequences, including prediction of signal peptide, molecular mass and isoelectric point, were carried out using the EXPASY proteomics server (http://www.expasy.org). The Weblogo online sever was used to identify the common elements in the R&R Consensus (RR-2) proteins (http://weblogo.berkeley.edu/logo.cgi).

2.3. Tissue-specific and developmental expression analysis of LmACP7

Total RNA was extracted using RNAiso™ Plus (Takara Bio, Kusatsu, Japan) from each of eight different tissues, including the wing pads (wings), integument, foregut, midgut, hindgut, Malpighian tubules, gonads and fat body from the 7-day-old fifth-instar nymphs and 2-day-old adults. For expression analysis of *LmACP7* at different development stages, we dissected the wing pads each 24 h after ecdysis from fourth instar nymphs to fifth-instar nymphs (24 h–168 h) and wings from adults emerge (ecdysis, 6 h, 12 h, 24 h, 28 h, 72 h, 96 h, and 120 h). Total RNA was extracted from each of these tissues. The quality and quantity of total RNA were evaluated on 1.5% agarose gels and NanoDrop 2000 (Thermo Fisher Scientific, Waltham, MA, USA). One μg of total RNA was used to synthesize first-strand cDNA by using M-MLV reverse transcriptase (Takara Bio, Kusatsu, Japan). Each cDNA sample was diluted 10-fold for reverse-transcription quantitative PCR (RT-qPCR) analysis. The RT-qPCR analysis was performed as described previously (Zhao et al., 2018), and relative mRNA levels of target genes were normalized to the expression of the internal marker gene, *RPL32,* that is stably expressed at all stages and in all tissues (Liu et al., 2013). At least three independent biological replicates were performed. The primers used are listed in Table S1.

2.4. Production of recombinant protein and western blotting analysis

The partial coding region of *LmACP7* was amplified with specific primers (Table S1, pET32a-A + 2/3B), and subcloned into pET32a vector (Novagen, Germany). The recombinant pET32a vector was used to transform *Escherichia coli* strain BL21 (DE3) cells (TransGen, Beijing, China) and induced by IPTG for expressing LmACP7 fusion protein with thioredoxin tag in N-terminal. The fusion protein was purified by using Ni-sepharose as described previously (Zhao et al., 2014). Purified protein (purity > 85%) was injected into New Zealand White rabbits for polyclonal antibody preparation, which was performed by Beijing Protein Innovation Co., Ltd.

Protein extracts were isolated from the wings, integument, gonads, fat body, Malpighian tubules, foregut, midgut, and hindgut from the 2-day-old adults. To further confirm the specific expression of LmACP7 in the nymphs at the protein level, we extracted the proteins from the wing pads, integument, gonads, fat body, Malpighian tubules, foregut, midgut, and hindgut from the 7-day-old fifth-instar nymphs. Western blotting was performed using polyclonal LmACP7 antibody as described previously (Zhao et al., 2014).

2.5. Immunohistochemistry

To localize LmACP7 protein in the wing pads and wings, immune staining was performed as described by Liu et al. (2009). In brief, paraffin sections (5 μm) of the wing pads from different days of fifth instar nymphs and the wings from the 2-day-old adults were prepared. The LmACP7 protein was detected in paraffin sections by incubation with the LmACP7 rabbit antiserum (1:200) as a primary antibody at 4 °C overnight followed by washing with PBS three times for 5 min each. The tissues were then incubated with Cy3-Affinipure Donkey Anti-Rabbit (Jackson ImmunoResearch, USA) secondary antibody for 1 h at room temperature. After washing the tissues three times with PBS, the specimens were incubated with Fluorescent Brightener 28 (FB28) (Sigma, USA) (1 mg/ml) for 5 s to detect chitin (Toprak et al., 2010). SYTOX^R Green nucleic acid stain (Life Technologies, USA) was added to label nuclei at a dilution of 1:50000. The stained tissues were imaged using an LSM 880 confocal laser-scanning microscope (Zeiss, Oberkochen, Germany) at 60× magnification. All the images in each staining experiment were collected under exactly the same conditions.

2.6. Immunogold staining

To determine the precise location of the LmACP7 protein in the wing cuticle of adult *L. migratoria*, immunogold labeling was performed using LmACP7 antibody. Ultrathin sectioned samples (~90 nm) were blocked with 0.01 M PBS (pH 7.4) containing 5% normal goat serum for 1 h, and then incubated with anti-LmACP7 rabbit antibody (1:20) in 0.05 M PBS containing 1% BSA and 0.02% TWEEN 20 for 2 h at room temperature. The tissues were rinsed with 0.01 M PBS three times for 5 min each and 0.05 M TBS (Tris-buffered saline) (pH 7.6) three times for 5 min each at room temperature followed by incubation with the secondary antibody conjugated with 10 nm gold particles (1:20) (Gold-conjugated Goat anti-rabbit IgG, BBI) in 0.05 M TBS (pH 8.0) containing 0.05% fish gelatin (BB International, Cardiff, UK) for 2 h at room temperature. The tissues were washed with 0.05 M TBS five times for 5 min each, deionized water four times for 5 min each at room temperature, and then stained with 4% aqueous uranyl acetate for 10 min. The images were captured with a JEM-1200 EX transmission electron microscope (TEM, JEOL, Japan).

2.7. Chitin binding assay

Five 5′-truncated fragments of the LmACP7 based on chitin binding domain (CBD) were generated by PCR from *LmACP17* cDNA using specific primers (Table S1), which were defined as pET32a-A + B + C, pET32a-A + B, pET32a-A + 2/3B, pET32a-A, and pET32a-B, respectively. Among them, pET32a-A + B + C, pET32a-A + B and pET32a-B contained the full-length of CBD (amino acids 50–102), whereas pET32a-A + 2/3B contained only part of CBD and pET32a-A contained no CBD. Amplified fragments were subcloned into pET32a vector (Novagen, Germany). The recombinant pET32a vectors were used to transform *E. coli* strain BL21 (DE3) cells (TransGen, Beijing, China) and induced by IPTG for expressing LmACP7 fusion proteins as described in section 2.4. The pET32a vector that expressed tag protein was used as control. The supernatants containing each recombinant protein were obtained after centrifugation of the homogenate of IPTG-induced *E. coli* cells that dissolved in 0.01 M PBS (pH 6.0) and were detected by SDS-PAGE analyses, and their concentrations were determined by BCA assays using BSA as a standard. The soluble proteins containing each recombinant protein were prepared for chitin-binding assay, and the final concentration was 1 μg/μl.

Colloidal chitin was prepared using shrimp shell chitin (Sigma, USA) as described by Shimahara (Shimahara and Takiguchi, 1988), and the final concentration was 1 μg/μl. Chitin binding was carried out according to the method of Deng et al. (2015) and Li et al. (2016) with slight modifications. After 700 μg soluble proteins (1 μg/μl) were incubated with 800 μl colloidal chitin at 4 °C for 12–20 h with shaking, the sample was centrifuged at 12000 g and 4 °C for 20 min. The supernatant was removed, and the precipitated chitin bound with proteins was washed with a washing buffer (0.01 M PBS, pH 6.0, 1 M NaCl), followed by centrifugation at 15000*g* and 4 °C for 20 min. The supernatants (unbound fractions) were removed and the pellets were saved as the P fraction (Two same samples were prepared). One of the pellets was resuspended in 50 μl of 1 × SDS-PAGE sample buffer for detecting by western blotting. Other pellets were then washed with 50 μl of 0.01 M sodium phosphate buffers (pH 8.0) for two times and centrifuged at 15000 g for 10 min to ensure that the non-specifically bound proteins were washed away from the chitin. The supernatants were saved as wash fractions (W1 and W2), and the pellet was re-suspended and washed with 50 μl of 0.01 M sodium phosphate buffers containing 1 M NaCl (pH 8.0) and 50 μl of 0.1 mol/L acetic acid (W3). The W1, W2 and W3 fractions were treated with the same volume of 2 × SDS-sample buffer for detecting by western blotting. Finally, 50 μl of 1 × SDS-PAGE sample buffer was added to the pellet and boiled for 5 min. The supernatant was collected by centrifuging the samples at 15000 g for 5 min as the bound fraction (E). SDS-PAGE (12% gel) was performed to analyze all the samples followed by western blotting with LmACP7 polyclonal antibody to detect the binding of CBD to colloidal chitin.

2.8. RNA interference (RNAi)

The forward and reverse primers harboring T7 RNA polymerase promoter sequences for synthesizing double-stranded RNA (dsRNA) of *LmACP7* (ds*LmACP7*) and *GFP* (ds*GFP*, control) genes were designed using the E-RNAi webservice (http://www.dkfz.de/signaling/e-RNAi3//) (Table S1). The dsRNA of *LmACP7* and *GFP* were synthesized using T7 RiboMAX™ Express RNAi System (Promega, Madison, WI, USA) as described previously (Zhao et al., 2018). The synthesized ds*LmACP7* and ds*GFP* were dissolved in appropriate volumes of deionized water, and the concentration was determined and adjusted to 2.5 μg/μl. The integrity of ds*LmACP7* and ds*GFP* was confirmed using agarose gel (2%) analysis. The 2-day-old fifth-instar nymphs were randomly divided into two groups (each with 30 nymphs) for injection of each dsRNA sample. Aliquots of 4 μl (10 μg) ds*LmACP7* or ds*GFP* were injected into the hemocoel between the second and third abdominal segments by using a microsyringe. The relative transcript levels of *LmACP7* were measured at 24 h after the injection of ds*RNA* by RT-qPCR as described above. Four biological replicates were applied for ds*GFP* and ds*LmACP7* injections. The remaining nymphs were maintained under the same conditions as described above. The visible phenotype changes were recorded every day until the nymphs started to molt to adults.

2.9. Mass spectrometry

To gain better silence efficiency and confirm the specificity of the LmACP7 antibody, the proteins were extracted from wing pads of the 7-day-old fifth-instar nymphs after treatment with *dsLmACP7* or ds*GFP* at day 2 of fourth-instar nymphs, and again at day 2 of fifth-instar nymphs. Proteins were homogenized in 100 μl of cold 0.01 M PBS (pH 7.4) containing a proteinase inhibitor cocktail. The homogenate was centrifuged at 13,000 × *g* for 10 min at 4 °C. The supernatant was collected as the PBS soluble fraction. The pellet was resuspended in 100 μl of SDS-PAGE sample buffer and then heated at 95 °C for 5 min followed by centrifugation at 13,000 × *g* for 5 min. The supernatant was collected as SDS-PAGE soluble fraction. The protein extracts were analyzed by 12% SDS-PAGE and detected by western bolting. The protein band selected from SDS-PAGE was excised and digested with trypsin, and the resulting fragments were analyzed by LC-MS/MS mass spectrometry as described previously (Yu et al., 2016).

2.10. Semithin section and transmission electron microscope (TEM)

The formation of mature wings and the dynamic structure of wing cuticle from fifth instar nymphs to adults were observed by semithin section and TEM analysis as the previously described method (Liu et al., 2009). Meanwhile, the cuticular structure of wing was also examined on day 2 of adults that treated with dsRNA at fifth instar nymphs by the same ways. The wing pads and wings were dissected from each of three locusts and fixed with 3% glutaraldehyde in 0.2 M phosphate buffer (pH 7.2) for 48 h at 4 °C. The samples were rinsed 3 times with the phosphate buffer followed by post-fixation in 1% osmium tetroxide for 3 h at 4 °C, and then the samples were washed twice, each for 10 min, and placed into a series of ascending concentrations of acetone (50, 70, 80, 90, and 100%) for dehydration. They were embedded in Epon 812 at room temperature for 2 h. Semithin sections (1 μm) were prepared, adhered to glass slides and stained with 1% (v/v) toluidine blue. Slides were observed with an optical microscope (OLYMPUS, Japan). For TEM analysis, Ultrathin sections (80 nm) prepared using a Reichert Jung ultramicrotome were collected on copper grids and counterstained with uranyl acetate and lead citrate. The images were captured with JEM-1200EX transmission electron microscope (TEM, JEOL, Japan).

2.11. Caspase activity

Caspase-3 and caspase-9 activities of pre-ecdysial wing pads of fifth-instar nymphs and post-ecdysis wings of adults after the treatment with ds*GFP* or ds*LmACP7* were analyzed using their respective activity kits, following the manufacturer's instructions (Beyotime, Shanghai, China).

2.12. TdT-mediated dUTP nick-end labeling (TUNEL)

Briefly, wing pads from dsRNA injection were collected in phosphate-buffered saline (PBS, 0.1 M, pH 7.2), fixed in 3% glutaraldehyde in 0.2 M phosphate buffer (pH 7.2) for 48 h at 4 °C, and washed three times with the PBS for 5 min. Paraffin sections of the wing pads after dsRNA injection were prepared as described in the section of immunohistochemistry. DNA fragmentation in wing pads was detected using the TdT-mediated dUTP nick-end labeling (TUNEL) kit (Beyotime Institute of Biotechnology, Shanghai, China) according to the manufacturer's instruction. The stained were imaged using an LSM 880 confocal laser-scanning microscope (Zeiss, Germany) at 60 magnifications. All the images in each staining were collected under the same conditions.

2.13. Staining of caspase-3 by immunohistochemistry

For detecting cleaved caspase-3 by immunohistochemistry, the paraffin sections of wing pads that treated with ds*GFP* or ds*LmACP7* were blocked in phosphate buffered saline containing 5% BSA and 0.1% Triton-X (PBST) for 1 h, and incubated with the cleaved caspase-3 antibody (BBI) at a dilution of 1:100 at 4 °C overnight. After washing three times with PBST, the samples were incubated with Alexa FlourR 488 Rabbit IgG (Life Technologies, USA) as secondary antibody (diluted 1:500) for 1 h at room temperature. DAPI (Sigma, USA) was added to label nuclei. Images were captured on an LSM 880 confocal laser-scanning microscope (Zeiss, Germany) at 60 magnifications equipped with a UV (405 nm) and a VIS (455 nm) laser to excite DAPI and Alexa FlourR 488 Rabbit IgG (Life Technologies, USA), respectively. All the images in each staining were collected under the same conditions.

2.14. RNA-seq

Total RNA was extracted from the wing pads of fifth-instar nymphs (pre-ecdysial) and the wings of the adults (24 h after ecdysis) that were treated with ds*GFP* or ds*LmACP7* on 2-day-old fifth-instar nymphs. For mRNA sequencing, mRNA was enriched and used to construct a cDNA library which was sequenced on an Illumina HiSeq2000 platform by Biomarker Technologies (Beijing, China). The raw sequences were trimmed to remove the adapters and poly(A/T) tails. The low-quality reads (Q20 less than 20) were also removed. The high-quality clean reads were then assembled to produce unigenes with the Trinity short read assembly program (Silvert et al., 1984). The assembled unigenes were aligned with the nr, nt, SwissProt, COG, and KEGG databases using BLAST with a cut-off *E*-value of 10^{-5}. Unigene abundance was measured by fragment per kilobase of exon per million fragments mapped (FPKM) and used for subsequent annotation and differential genes expression analysis. The differential genes were detected by RT-qPCR as described above.

2.15. Statistical analysis

All data were statistically analyzed by independent sample Student *t*-test. Asterisks indicate significant differences (*, $P < 0.05$; **, $P < 0.01$; ***, $P < 0.001$).

3. Results

3.1. Formation and dynamic structure of mature wings from fifth instar nymph to adult

Insect wings are composed of two monolayers (ventral and dorsal) of epithelial cells that secrete lower and upper cuticular laminae, respectively. The development of mature wings from nymph to adult locusts was detected by semi-thin sections. In early stages of wing pad formation in fifth-instar nymphs (24 h–96 h), the space between lower and upper cuticular layers was narrow (Figs. S1A–D). During wing pad apolysis at about 120 h (Fig. S1E), the old cuticle was degraded and the new cuticle was synthesized (Figs. S1F–G). After ecdysis, the newly formed adult wings consisted of veins and a wing membrane with a broader space between lower and upper cuticular layers (Fig. S1H). The space was then gradually compressed until the mature flat wings were formed (Fig. S1I-L).

Based on the ultrastructure from our TEM analysis (Fig. 1), the cuticle of wing pads consisted of only the epicuticle and exocuticle in newly molted fifth-instar nymphs (N5-0 h). After molting, the endocuticle formation was initiated and the cuticle was fully formed within about 96 h (N5-96 h) after ecdysis (Fig. 1A–E). Before molting to adult, the cuticle of wing pads began to undergo apolysis at about 120 h (Fig. 1F), thereafter the old cuticle was degraded. Concomitantly, the new adult cuticle (epicuticle and exocuticle) was synthesized (Fig. 1G–H), and the endocuticle of adult wings gradually thickened from 0 h to 48 h after ecdysis (Fig. 1I–M).

3.2. Identification and characterization of LmACP7 from locust wing pads

In a previous study, we identified a cuticle protein gene *LmACP7,* which was highly expressed in wing pads of nymphs Zhao et al., 2017. From the *L. migratoria* wing pads transcriptome (GBDZ00000000) and the genomic data of *L. migratoria* (AVCP00000000), we assembled the intron/exon organization of *LmACP7*, which consisted of three exons spanning a 509-bp coding region (Fig. S2A). The open reading frame was 441 bp and encoded a protein of 147 amino acid residues containing a putative signal peptide sequence (amino acids 1–16) and a RR-2 motif (amino acids 43–108, containing a chitin binding domain 4 (CBD, amino acids 50–102), S2B-C) with a theoretical molecular mass and pI of 15.1 kDa and pKa 5.9, respectivelyFig. S2B. LmACP7 is rich in alanine (26.5%), valine (10.9%) and proline (8.8%), probably conferring an unordered protein structure besides the RR-2 motif.

3.3. LmACP7 is expressed specifically in wings and is a pre-ecdysial protein

In order to determine the tissue-specific expression of *LmACP7*,

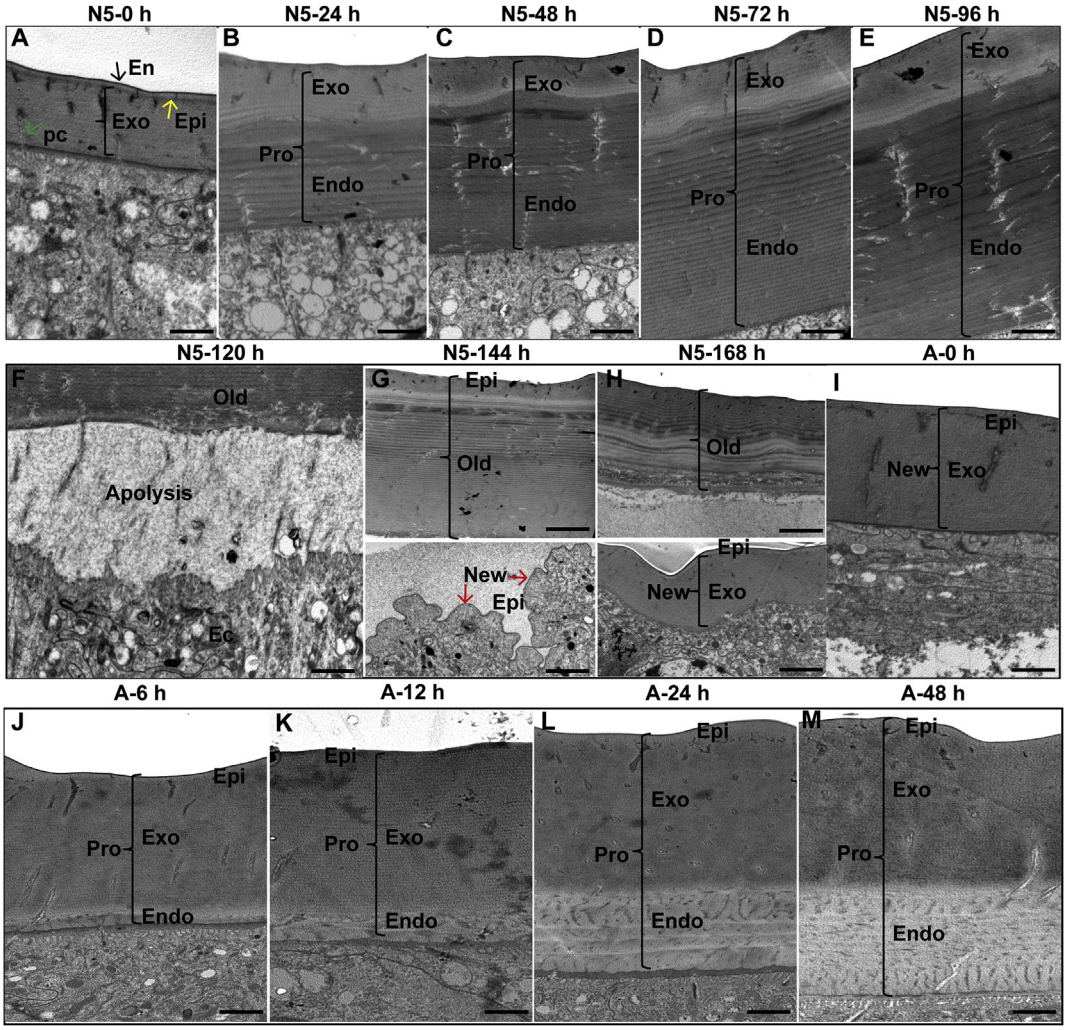

Fig. 1. Formation of exocuticle and endocuticle in *L. migratoria* during wing pad-wing transition by TEM
A-E. Formation of endocuticle of wing pad was observed at different development stages of fifth instar nymphs by TEM. **F–H.** Apolysis, degradation of old cuticle and forming of new cuticle (epicuticle and exocuticle) in later fifth-instar stages. **I-M.** Formation of endocuticle in adult wing. N5: fifth-instar nymph wing pads, A: Adult wing, Epi: Epicuticle, Pro: Procuticle, Exo: Exocuticle, Endo: Endocuticle, Old: old cuticle, New: new cuticle, red arrow indicates new cuticle, Scale bar = 2 μm. (For interpretation of the references to colour in this figure legend, the reader is referred to the Web version of this article.)

different tissues collected on 2-day-old adults were analyzed at the mRNA level by RT-qPCR. The results showed that *LmACP7* was highly expressed in the wings, but little or no expression was detected in integument and other tested tissues except the fat body (Fig. 2A). To verify the tissue-specific expression of LmACP7 at the protein level, Western blot analysis was performed using extracts of different tissues from 2-day-old adults probed with a LmACP7-specific antibody. As shown in Fig. 2, LmACP7 was detected in adult wings, trace amounts in the fat body, but not in other tissues (Fig. 2B).

As mentioned above, the theoretical molecular mass of LmACP7 is about 15.1 kDa. However, in Western blot experiments, we detected a > 43 kDa protein in both the wing pads and the adult wings (Fig. 2B), which is not consistent with the predicted molecular mass. To test the specificity of our LmACP7 antibody, we silenced the expression of *LmACP7* by injecting dsRNA for *LmACP7* (ds*LmACP7*) on day 2 of fourth-instar nymphs, and again on day 2 of fifth-instar nymphs. The nymphs injected with the dsRNA for *GFP* (ds*GFP*) was used as control under the same conditions. Total RNA and proteins were extracted from fifth-instar nymphs before ecdysis following the injection of ds*LmACP7* and ds*GFP*. The RT-qPCR results showed that the expression level of *LmACP7* was substantially suppressed in the ds*LmACP7*-injected nymphs with a silencing efficiency higher than 96% compared with that of the control (Fig. S3A). To identify LmACP7, proteins from the fifth-instar nymphs injected with ds*LmACP7* and ds*GFP* were separated by SDS-PAGE, and detected by western bolting. Our results showed that there was a 43 kDa protein present in extracts from ds*GFP*-injected nymphs but absent in extracts from ds*LmACP7*-injected nymphs (Fig. S3B). The band from control extracts was identified by mass spectrometry by searching the transcriptome database established in our lab. Our results showed the presence of LmACP7 in the gel (Figs. S3C and D), suggesting that the LmACP7-specific antibody recognizes LmACP7.

To verify the tissue specificity of LmACP7 at the nymphal stage, *LmACP7* expression was examined in different tissues at day 7 of fifth-instar nymphs by RT-qPCR. *LmACP7* was highly expressed in the wing pads of fifth-instar nymphs, but little or no expression was detected in other tested tissues (Fig. S4A). The results from Western blot analysis were consistent with the mRNA expression pattern (Fig. S4B), and the expression of *LmACP7* between forewing and hindwing is not markedly different at both mRNA and protein levels (Figs. S4C–D). To explore stage-specific expression patterns of *LmACP7*, the temporal expression patterns of *LmACP7* mRNA in wing pads from fifth-instar nymphs and the wings of adults were analyzed using RT-qPCR. *LmACP7* mRNA was detected at a low expression level at early stages (24 h–96 h) and at the stages of apolysis and formation of the new cuticle (120 h–144 h).

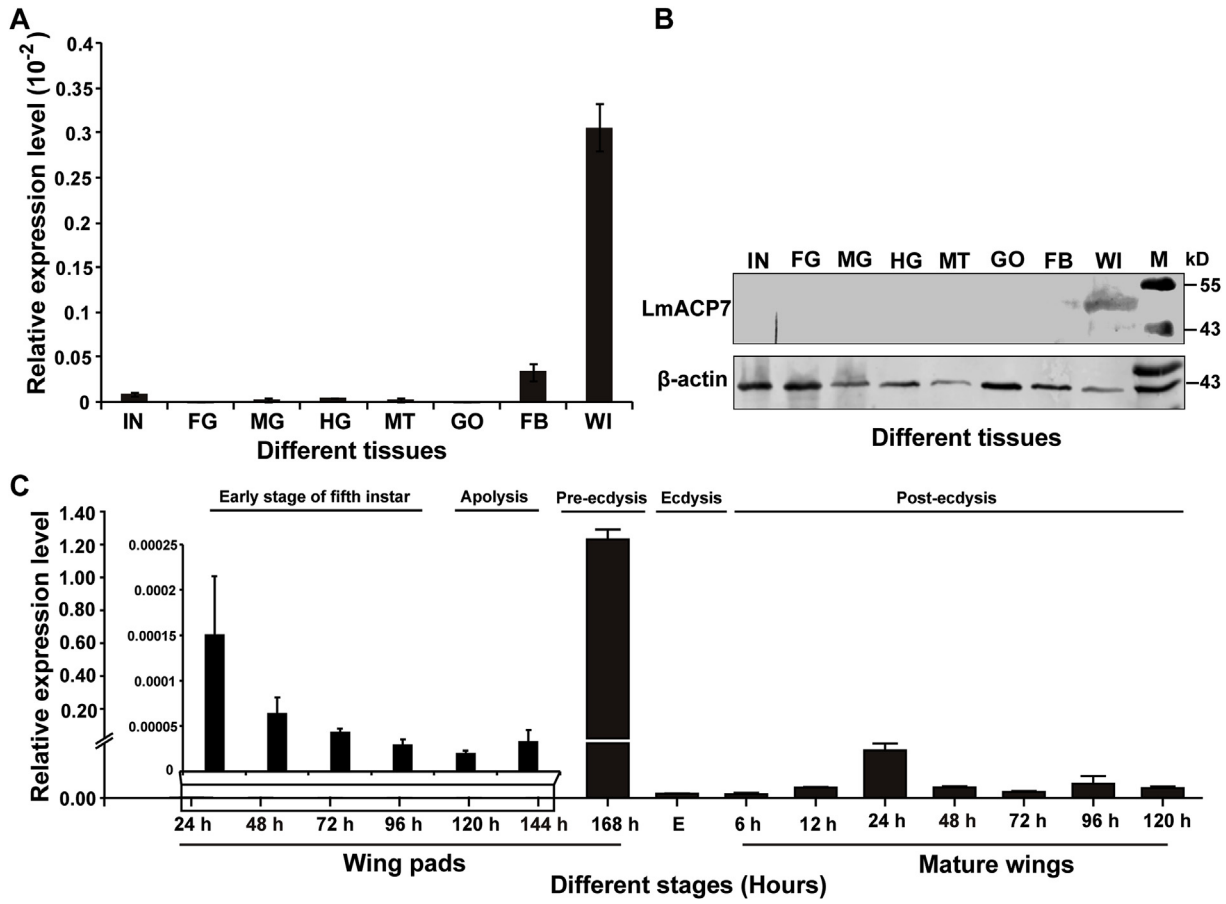

Fig. 2. Expression of *LmACP7* in different tissues of adults and during the development of fifth-instar nymphs to adults in *L. migratoria*.
A. Expression of *LmACP7* in different tissues of adults as detected by RT-qPCR. *RPL32* was used as the reference control. All data are reported as means ± SE of three independent biological replications. **B.** LmACP7 protein in different tissues of adult was detected by Western blot experiments. β-actin was used as the reference control. 200 μg total proteins were used in each line. Different tissues are listed: IN, Integument; FG, foregut; MG, midgut; HG, hindgut; GO, gonad; MT, Malpighian tubules; FB, fat body; WI, wings. **C.** Expression of *LmACP7* in different stages (from fifth instar nymph to adult) as detected by RT-qPCR. *RPL32* was used as the reference control. All data are reported as means ± SE of three independent biological replications. E: ecdysis.

Expression levels increased at pre-ecdysis (168 h) of fifth-instar nymphs, followed by a sharp decrease at ecdysis. Expression levels again slightly increased between 6 h and 24 h after ecdysis (Fig. 2C).

3.4. *LmACP7 is transported from epidermal cells to exocuticle during wing pad-wing transition*

To analyze the localization of LmACP7 during the development of nymphs' wing pads to adult wings, we performed immunohistochemistry experiments on paraffin sections of wing pads prepared at different time points during the fifth-instar nymphal stage and of the wings from 2-day-old adults. As shown in Fig. S5, the cuticle of wing pads underwent apolysis at 120 h, and the new cuticle started to be formed between 120 h and 144 h (Fig. S5A-B and A'-B'). Thereafter, LmACP7 began to accumulate in the newly formed cuticle and co-localized with chitin at 168 h (Fig. S5A-C and A'-C'). The new adult wing cuticle was composed of the epicuticle and the exocuticle. After molting, LmACP7 was mainly detected and co-localized with chitin in the exocuticle of the wing, but little signal was found in epidermal cells (Fig. 3A–C'). To determine the location of LmACP7 in the wing cuticle more precisely, we used an immunogold labeling technique and examined the protein localization by TEM. In the wing veins, LmACP7 was detected throughout the exocuticle but not in the endocuticle (Fig. 3D–D'). Similar localization and distribution of LmACP7 were also observed in the wing membrane (Fig. 3E–E' and F-F'). In control experiments, there were no or little signal in the wing cuticle and epidermal cell after RNAi with injection of ds*LmACP7* (Fig. 3G–G'').

3.5. *LmACP7 binds to chitin in vitro*

To confirm the chitin-binding activity of LmACP7, five 5′-truncated LmACP7 fragments (pET32a-A + B + C, pET32a-A + B, pET32a-A + 2/3B, pET32a-A and pET32a-B) were generated as described in methods and materials section (Fig. S6A). The soluble proteins were used for chitin-binding assay. Soluble protein obtained from pET32a vector was used as control. Our results showed that the LmACP7 protein and those proteins harboring the CBD peptide (pET32a-A + B + C, pET32a-A + B, and pET32a-B) were able to bind chitin *in vitro* (Fig. S6B, line 1–2 and line 5), whereas those proteins and the control devoid of the CBD peptide (pET32a-A + 2/3B, pET32a-A and pET32a) failed to do so (Fig. S6B, lanes 3–4 and 6). These results suggest that the predicted chitin-binding domain is required for LmACP7 to bind chitin.

3.6. *LmACP7 is required for the formation of wing*

To investigate the function of LmACP7, we examined the morphology of the wings in adults during nymph-adult molt after the *LmACP7* transcript level was suppressed by RNAi. Injection of dsRNA targeting *LmACP7* expression in 1-day-old fifth-instar nymphs suppressed its transcript level in the wing pads by 95% at day 7 as determined by RT-qPCR and reduced its protein level significantly at day 7 as revealed by western blotting (Fig. 4A–B). Injection of ds*LmACP7*

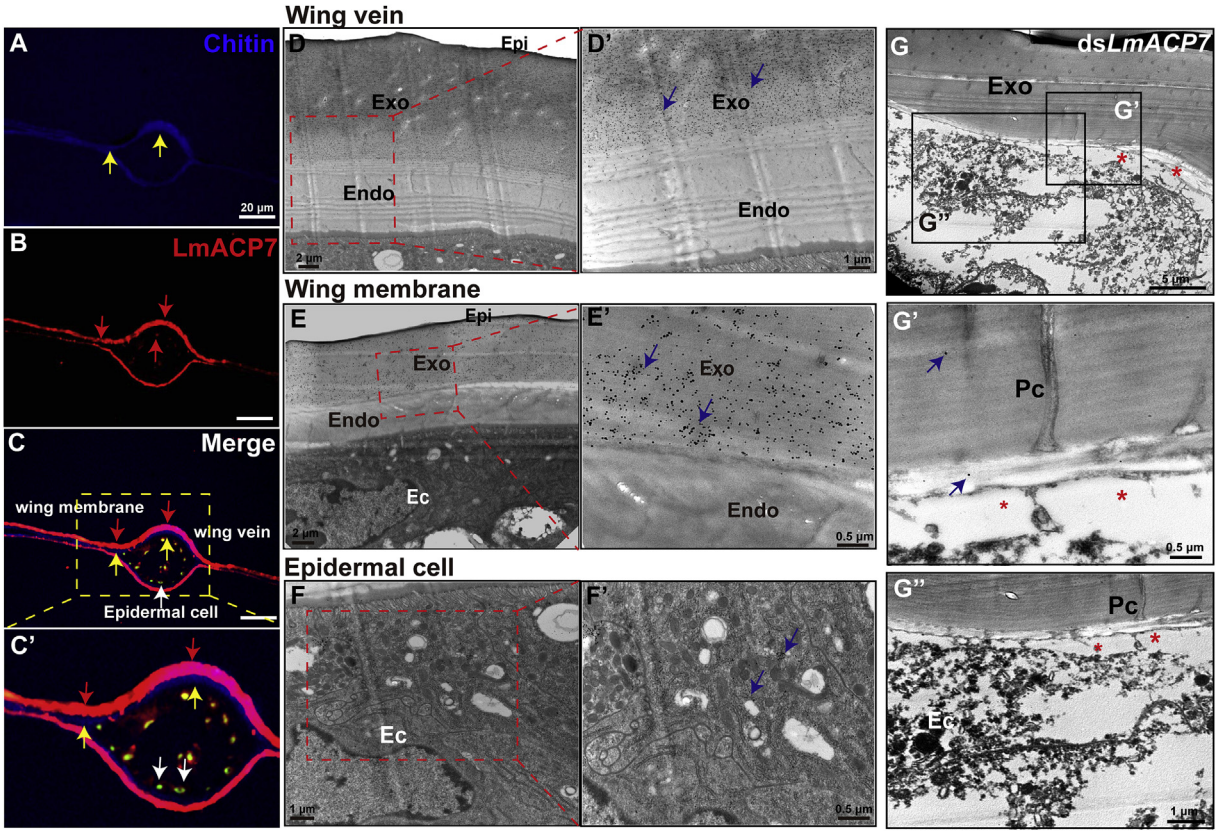

Fig. 3. Localization of LmACP7 in *L. migratoria* wings by immunochemistry and immunogold labeling.
A-C. Localization of LmACP7 in adult wings of *L. migratoria* by immunochemistry, Scale bar = 20 μm; SYTOX^{R} Green nucleic acid stain, Nucleus, FB28, Chitin; LmACP7: Anti-LmACP7. The red arrows indicate LmACP7 signal in cuticle and cytoplasm. The white arrows indicate epidermal cells, and the yellow arrows indicate chitin signal, Scale bar = 20 μm. The stained sections were imaged using an LSM 880 confocal laser-scanning microscope (Zeiss, Germany) at 60× magnification. All the images for each staining experiment were collected under the same conditions. **D-F.** Precise localization of LmACP7 in adult wing of *L. migratoria* by immunogold labeling. G-G''. As a control, localization of LmACP7 in adult wing of *L. migratoria* by immunogold labeling after RNAi by injection of ds*LmACP7*. Epi: Epicuticle, Endo: Endocuticle, Exo: Exocuticle, Ec: Epithelial cells, Pc: Pore canal. Blue arrow indicates gold particles, red asterisks indicate the space caused by loss of LmACP7 and the detachment of the cuticle from epithelial cells. (For interpretation of the references to colour in this figure legend, the reader is referred to the Web version of this article.)

into nymphs caused wing defects (in about 56% of injected insects) during nymph-adult transition. In particular, the wings were wrinkled and did not elongate fully failing to extend far enough to cover the entire abdomen (Fig. 4C–C'). The results of semi-thin sections showed that compared to ds*GFP*-treated control insects, the ventral and dorsal cuticles of mature forewings and hindwings from ds*LmACP7*-injected insects did not adhere to each other to form the normal wing veins and wing membranes (Fig. 4D–D' and Fig. S7A-A').

To gain a better understanding of the ultrastructure and morphology of wing cuticle, we also performed TEM of wing cuticle from the dsRNA-treated insects. In both the veins and wing membranes of ds*GFP*-treated control, the cuticle consists of the envelope, the epicuticle and the procuticle that contain chitin lamellae subdivided into an exocuticle and an endocuticle (Fig. 4E–F, and Figs. S7B–C). However, it was found that the lamellae in the region connecting the endocuticle and the apical plasma membrane of epidermal cells was disordered, and the microvilli were degraded to different extents. Although the adult exocuticle had a normal thickness and structure including pore canals in the wing veins, the thickness of the endocuticle was dramatically decreased in the ds*LmACP7*-treated insects compared to ds*GFP*-treated control insects (Fig. 4E'-F' and Fig. S7B'-C'). These results indicated that LmACP7 is needed for structural integrity of the wings cuticle during nymph-adult molt.

3.7. Deficiency of LmACP7 promotes cell death during nymph-adult molting

Taking all these results into consideration, we propose a hypothesis that LmACP7 is a major structural protein in the wing exocuticle, which is required for the stability of adult wing epithelial cells. To test this hypothesis, we first observed the structure of wing epithelial cells before ecdysis by TEM. The results showed that in both ds*GFP*-treated control insects and ds*LmACP7*-treated insects, the apical plasma membranes of epithelial cells in wings form short microvilli, which possess electron-dense plaques at their tips, and there are visible cell junctions by which epithelial cells are held together, endoplasmic reticulum (ER), mitochondria and a nucleus (Fig. 5A–A'' and B-B''). However, after ecdysis, the wing epithelial cells from ds*LmACP7*-injected insects exhibited cell debris, and the microvilli, ER, mitochondria and cell junctions were degraded to different extents and the morphological characteristics of cell death such as pyknosis and karyorrhexis usually observed during apoptosis became apparent (Fig. 5C–C'' and D-D'').

Did LmACP7 deficiency induce the disorder of epithelial cells that underwent an apoptosis-like cell death during molting? To assess this possibility, we assayed caspase activity, a marker of apoptosis. These assays revealed that both caspase-3 and caspase-9 activities dramatically increased in the ds*LmACP7*-treated insects compared to the ds*GFP*-treated control after ecdysis (Fig. 6A), but were unchanged in both ds*LmACP7*-treated and ds*GFP*-treated control animals before ecdysis (Fig. 6B). To detect the molecular changes that occurred in the period of ecdysis, RNA-seq analysis was performed using the wing pads from fifth

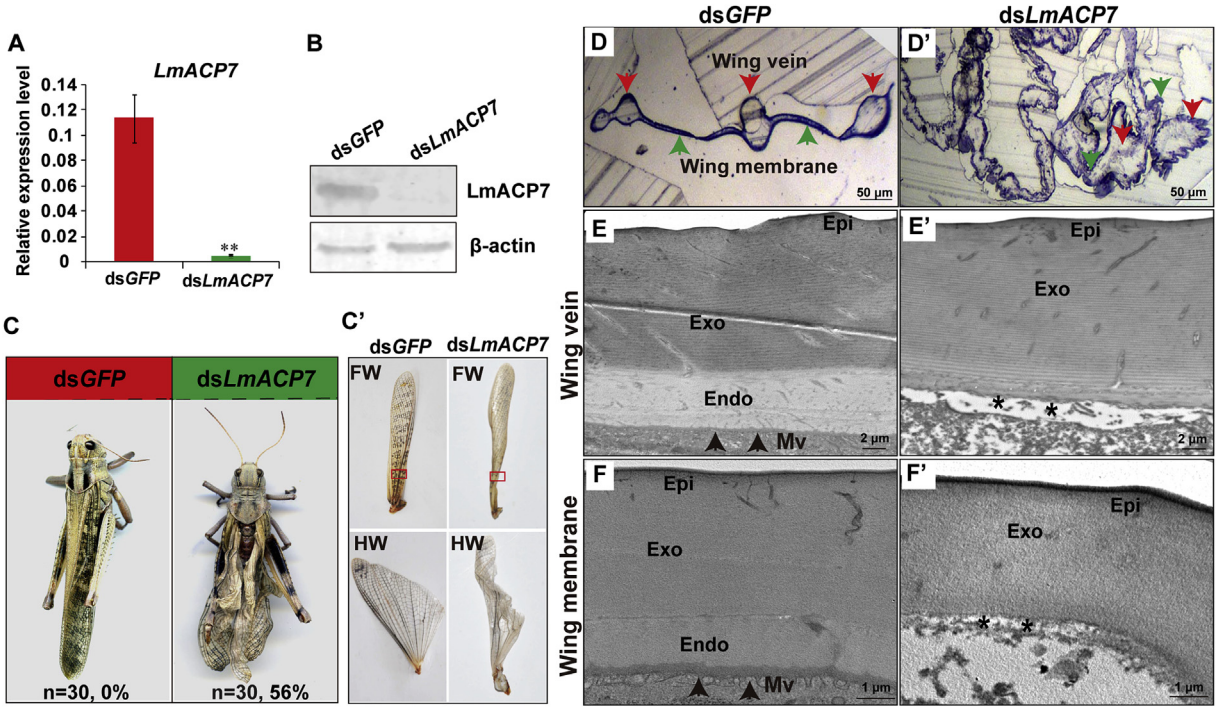

Fig. 4. Effect of ds*LmACP7* RNAi on structure of adult wings of *L. migratoria*

A. Expression of *LmACP7* after RNAi as detected by RT-qPCR. *RPL32* was used as the reference control. Data are reported as means ± SE of three independent biological replications; asterisks indicate significant differences, **, $P < 0.01$. **B.** LmACP7 protein in the RNAi insects was detected by Western blot using LmACP7 antiserum; **C–C'.** The phenotypes of adults and wings (forewing (FW) and hindwing (HW)) were observed after RNAi in fifth instar nymphs. N = 30, indicating number of individuals. **D-D'.** The anatomical structure of the forewing was observed after RNAi by TEM of semi-thin sections. Red arrow indicates wing vein, green arrow indicates wing membrane. **E-E′ and F–F'.** The structure of adult forewing was observed after RNAi in fifth instar nymphs through TEM. En: Envelope, Epi: Epicuticle, Endo: Endocuticle, Exo: Exocuticle, Ec: Epithelial cell. Scale bar = 2 μm (E and F); Scale bar = 1 μm in E′ and F'. Black arrows indicate microvilli. (For interpretation of the references to colour in this figure legend, the reader is referred to the Web version of this article.)

instar nymphs (24 h pre-ecdysial) and wings from adults (24 h after ecdysis) that had been treated with ds*GFP* or ds*LmACP7* when they were 2 days old fifth instar nymphs. In ds*LmACP7*-treated insects before ecdysis and after ecdysis, we identified 274 and 146 differentially expressed genes (DEGs), respectively, when compared to the control. Among these genes, 217 genes were down-regulated and 57 were up-regulated before ecdysis, while 66 genes were down-regulated and 80 genes were up-regulated after ecdysis (Fig. 6C). In addition, 5091 DEGs (2652 up-regulated and 2439 down-regulated) were identified in the ds*GFP*-treated animals after ecdysis compared to the ds*GFP*-treated insects before ecdysis (Fig. 6C). Among these, expression levels of the cell junction related gene *Nectin*, the cell polarity related gene *Arm*, the hippo pathway gene *Yorkie* and the cell cycle gene Cyclin E (*CyclE*) were lower in the ds*LmACP7*-treated insects compared to ds*GFP*-treated insects after ecdysis. These genes did not show any expression differences between ds*LmACP7*-treated and ds*GFP*-treated control insects before ecdysis according to the transcriptome data and RT-qPCR results (Fig. 6D–E). In addition, we found in RT-qPCR experiments that cell polarity related genes (*Coracle*, *Crumbs*, *Dachsous*, *Dlg-5* and *Dlg-1*), and Hippo pathway genes (*Warts*, *Merlin*, *Expanded*, and *Hippo*) were suppressed in ds*LmACP7*-treated insects compared to ds*GFP*-treated control insects after ecdysis, while, by contrast, no significant differences were observed in the transcriptome data for these genes in respective insects (Fig. 6D–E). This discrepancy may reflect sensitivity differences of the applied methods. Furthermore, the mRNA abundance of apoptosis regulator and initiator genes (*ICE1*, *ALG2*, and *CASP9*) were dramatically up-regulated, whereas the mRNA level of apoptosis inhibitor genes (*IAP* and *Blc-2*) were dramatically down-regulated in the ds*LmACP7*-treated insects compared to the ds*GFP*-treated control insects after ecdysis, but no expression differences for these genes were observed in both ds*LmACP7*-treated and ds*GFP*-treated control insects before ecdysis (Fig. S8A). The expression of a gene encoding apoptotic protease-activating factor, *Apaf1*, was also significantly increased in the ds*LmACP7*-treated insects compared to ds*GFP*-treated control insects after ecdysis by RT-qPCR, while no significant expression difference for these gene was found in the transcriptome data (Fig. S8A). In order to further test the hypothesis that deficiency of LmACP7 induces an apoptosis-like cell death, we performed TUNEL staining and immunohistochemical analysis with an antibody against cleaved caspase 3 (an apoptotic effector) after ecdysis of fifth instar nymphs injected with ds*LmACP7* or ds*GFP* on day 2 of fourth instar nymphs. Of note, because adult wings are fragile, they are difficult to handle, therefore the wing pads of nymphs were chosen to be examined for this experiment. An apoptosis-like process was detected in ds*LmACP7*-injected nymphs, but was undetectable in ds*GFP*-treated control nymphs (Fig. S8B). As revealed by immunohistochemistry, cleaved caspase-3 was detected in the nuclei of epithelial cells of ds*LmACP7*-injected nymphs (Fig. S8C). Also, caspase-3 activity and its mRNA levels were increased approximately 30% and 50% in ds*LmACP7*-injected nymphs compared with ds*GFP*-treated control insects, respectively (Fig. S8D). These results support the hypothesis that LmACP7 suppression promotes an apoptosis-like cell death during molting.

3.8. Deficiency of LmACP7 leads to decline in the expression of post-ecdysis CP genes

Based on the results of RNA-seq analysis, we identified five pre-ecdysis *CP* genes (CPR family genes *LmACP19* and *LmNCP19.8*, *LmNCP21.3*, *hypothetical CP*, and *CPAPs* family gene *LmObst-F*) and five post-ecdysis CP genes (CPF family genes *LmCP2* and *LmCP6*, Endocuticle structural glycoprotein genes *LmAbd2* and *LmAbd8,* and *putative CP*) that are highly expressed in wing pads and adult wings

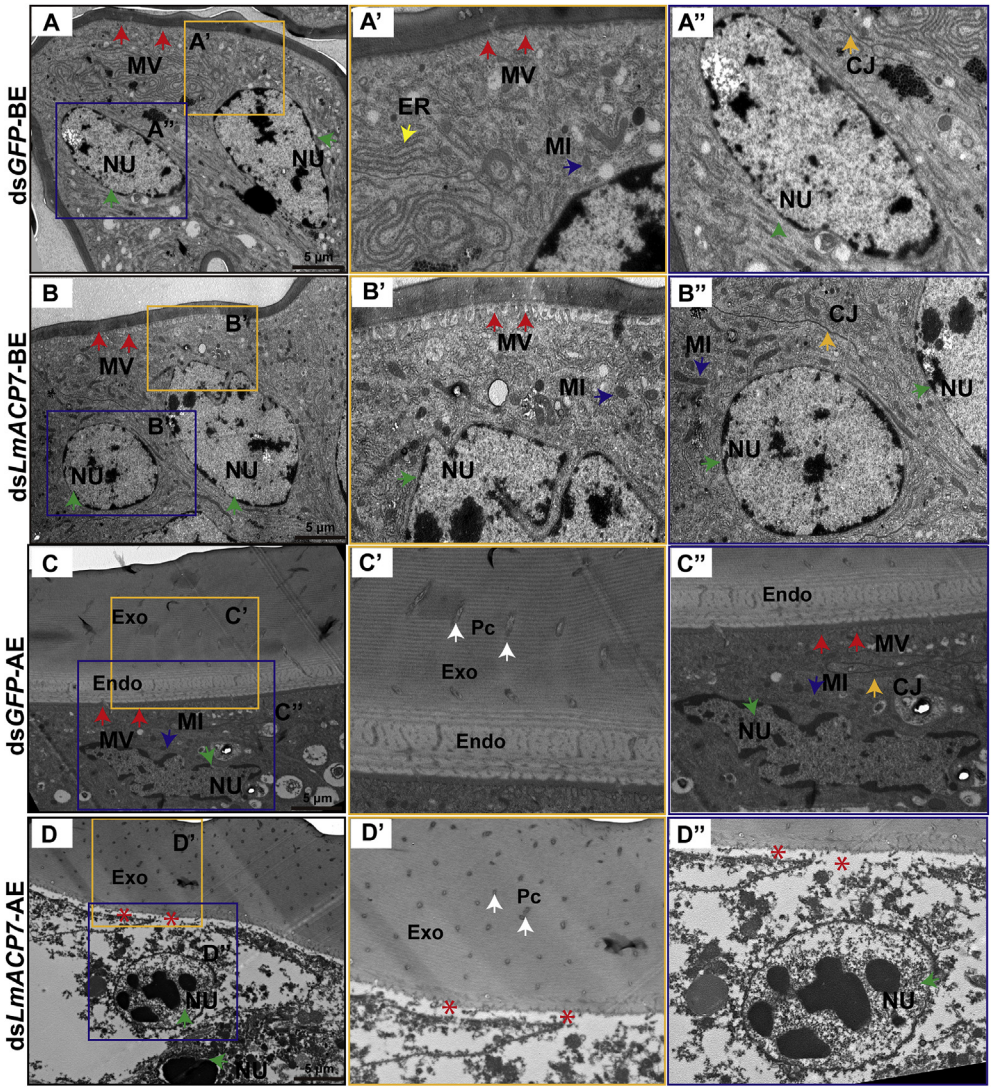

Fig. 5. Deficiency of *LmACP7* promotes apoptosis or apoptosis-like response in wings after ecdysis.
A-B. The structure of wing pad before ecdysis was observed after RNAi in fifth instar nymphs through TEM, Scale bar = 5 μm. **C-D.** The structure of adult wings after ecdysis were observed after RNAi in fifth instar nymphs through TEM. Scale bar = 5 μm. Red arrow indicates microvilli (MV), yellow arrow indicates cell junction (CJ), green arrow indicates nucleus (NU), White arrow indicates pore canal (Pc), the blue arrow indicates mitochondria (MI), red asterisks indicate the space that loss of LmACP7 leads to detachment of the cuticle from epithelial cells. A′, B′, C′, D′ and A", B", C" and D" are larger magnifications of regions indicated by yellow and blue rectangles. (For interpretation of the references to colour in this figure legend, the reader is referred to the Web version of this article.)

(Fig. 7A–B). RT-qPCR results showed that *LmACP19*, *LmNCP21.3*, and *LmNCP19.8* are highly expressed before ecdysis, but at lower levels at ecdysis and after ecdysis. These are pre-ecdysial protein genes that may be involved in the formation of the exocuticle (Fig. 7C). In contrast, *LmCP2*, *LmCP6* and *LmAbd2* are highly expressed during ecdysis and after ecdysis, but at lower levels before ecdysis, thereby representing genes encoding post-ecdysial proteins (Fig. 7D) that are possibly involved in the formation of the endocuticle. After deficiency of *LmACP7* by RNAi injected on day 2 of fifth instar nymphs, the expression of *LmACP19*, *LmNCP19.8* and *LmNCP21.3* is dramatically increased, but that of *LmObst-F* is dramatically decreased before ecdysis (Fig. 7E). By contrast, the expression of *LmCP2*, *LmAbd2* and *LmAbd8* are dramatically decreased in the ds*LmACP7*-treated insects after ecdysis compared to ds*GFP*-treated insects (Fig. 7F). These results suggest that deficiency of *LmACP7* may decline the expression of post-ecdysis protein genes and upregulate the expression of pre-ecdysis genes during molting.

4. Discussion

4.1. LmACP7 is a wing-specific cuticular protein expressed during pre-ecdysial period

The CPR subfamily proteins with the R&R consensus that confers chitin-binding properties, is the largest arthropod cuticular protein family. According to our previous studies, the CPR family is also the largest family of cuticle proteins in the migratory locust (Zhao et al., 2017), which contains three subgroups (RR-1, RR-2 and RR-3). Several wing-specific cuticle proteins belonging to this family were identified. Among them, *LmACP7* that encoded a protein belonging to the RR-2 subgroup of CPR family was specifically expressed in the nymph wing pads at the transcript level (Zhao et al., 2017). In the present study, we have demonstrated that its expression is wing-specific at the mRNA and protein levels using RT-qPCR and western blotting (Fig. 2A and B). It is specifically expressed at the pre-ecdysial stage (Fig. 2C). It accumulates in the exocuticle as shown by immunogold labeling with a specific antibody (Fig. 3 D' and E'). As reported by other groups, the proteins belonging to subgroup RR-1 are mainly present in soft, flexible, hydrated cuticles, such as larval cuticles in Diptera and Lepidoptera and in intersegmental membranes and the endocuticle in locusts. By contrast, the members of subgroup RR-2 have mainly been found in cuticles, which tend to be stiff and sclerotized, such as larval and adult cuticle of *Tenebrio molitor* (Charles et al., 1992), elytra and hindwing cuticle of *T. castaneum* (Dittmer et al., 2012; Noh et al., 2017), adult pharate cuticle from *Locusts* (Klarskov et al., 1989; Krogh et al., 1995), pupal cuticle of *D. melanogaster* (Apple and Fristrom, 1991), and larval and pupal cuticle of *Hyalophora cecropia* (Lampe and Willis, 1994). Thus, a hypothesis was proposed that a correlation exists between the type of proteins and mechanical properties of the cuticles. However, in *Anopheles gambiae*, immunolocalization analysis indicated that the location of RR-1 proteins and RR-2 proteins depends more on properties of

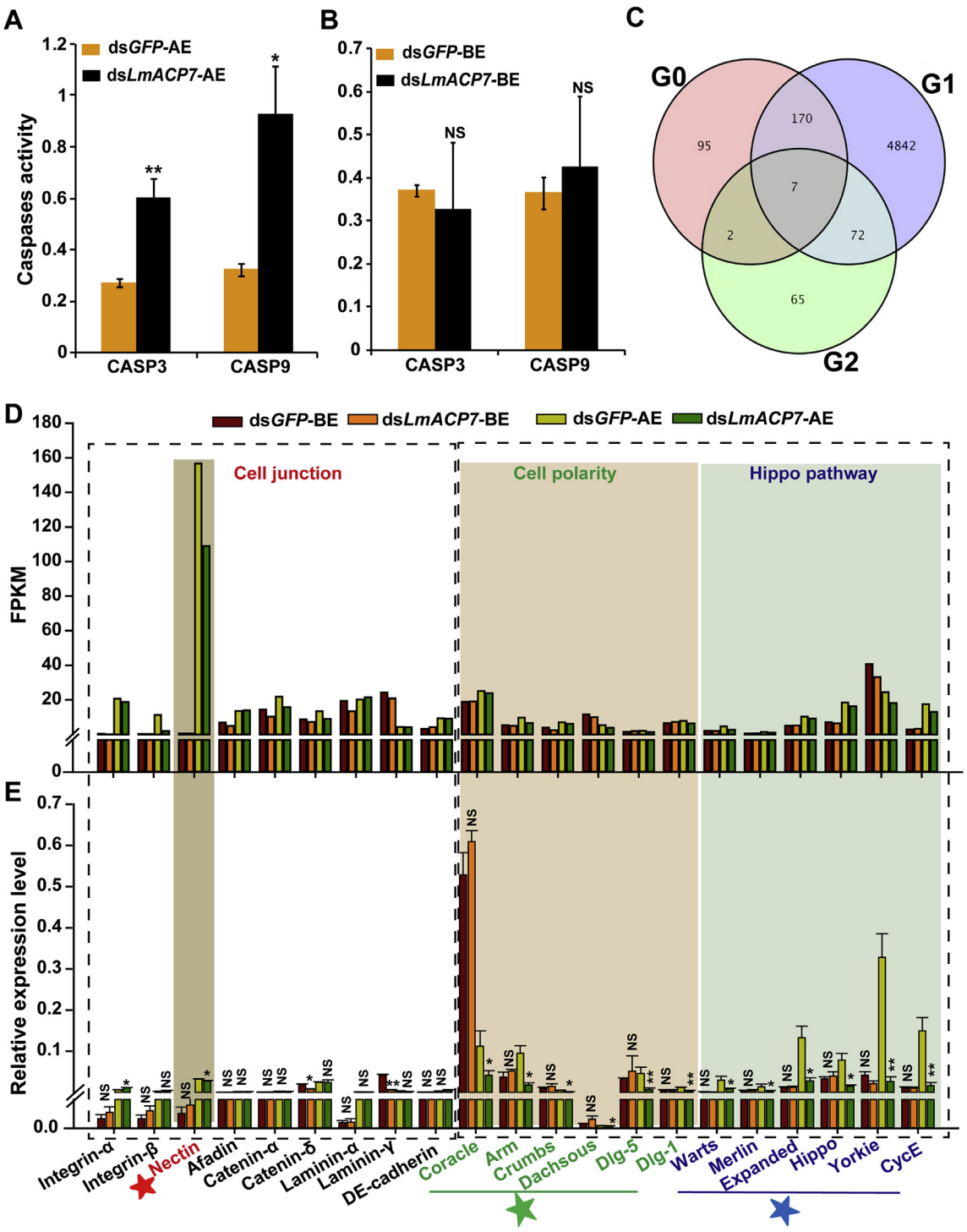

Fig. 6. Activity of caspases and differential expression of genes in both pre- and after ecdysis by RNA-seq.
A-B. Activity of caspase-3 and caspase-9 were detected in extracts of insects before ecdysis and after ecdysis after RNAi initiated by injection of ds*LmACP7* or ds*GFP* on day 2 of fifth instar nymphs. *RPL32* was used as the reference control. Data are reported as means ± SE of three independent biological replications; asterisks indicate significant differences, *, $P < 0.05$, **, $P < 0.01$. **C.** Venn diagram of differential expression of genes between ds*LmACP7*- and ds*GFP*-treated insects sampled before or after ecdysis. G0: ds*GFP*-BE & ds*LmACP7*-BE, G1: ds*GFP*-BE & ds*GFP*-AE, G2: ds*GFP*-AE & ds*LmACP7*-AE. **D.** The cell junction, cell polarity, and hippo pathway related genes were identified based on the transcriptome data. **E.** The cell junction, cell polarity, and hippo pathway related genes were determined at before ecdysis and after ecdysis after injection of ds*LmACP7* or ds*GFP* on day 2 of fifth instar nymphs. *RPL32* was used as the reference control. Data are reported as means ± SE of three independent biological replications; asterisks indicate significant differences, *, $P < 0.05$, **, $P < 0.01$, NS indicate no significantly difference. BE: before ecdysis; AE: after ecdysis.

individual proteins than on the hypothesis (Vannini and Willis, 2017). In *L. migratoria*, LmACP7 belongs to the RR-2 subgroup of CPR family and is located in the exocuticle of wings (Fig. 3). When *LmACP7* was knocked down by RNAi, the resulting adult wings were not fully elongated but remained wrinkled (Fig. 4), implying that LmACP7 may be involved in the maintenance of the structural integrity of adult wings.

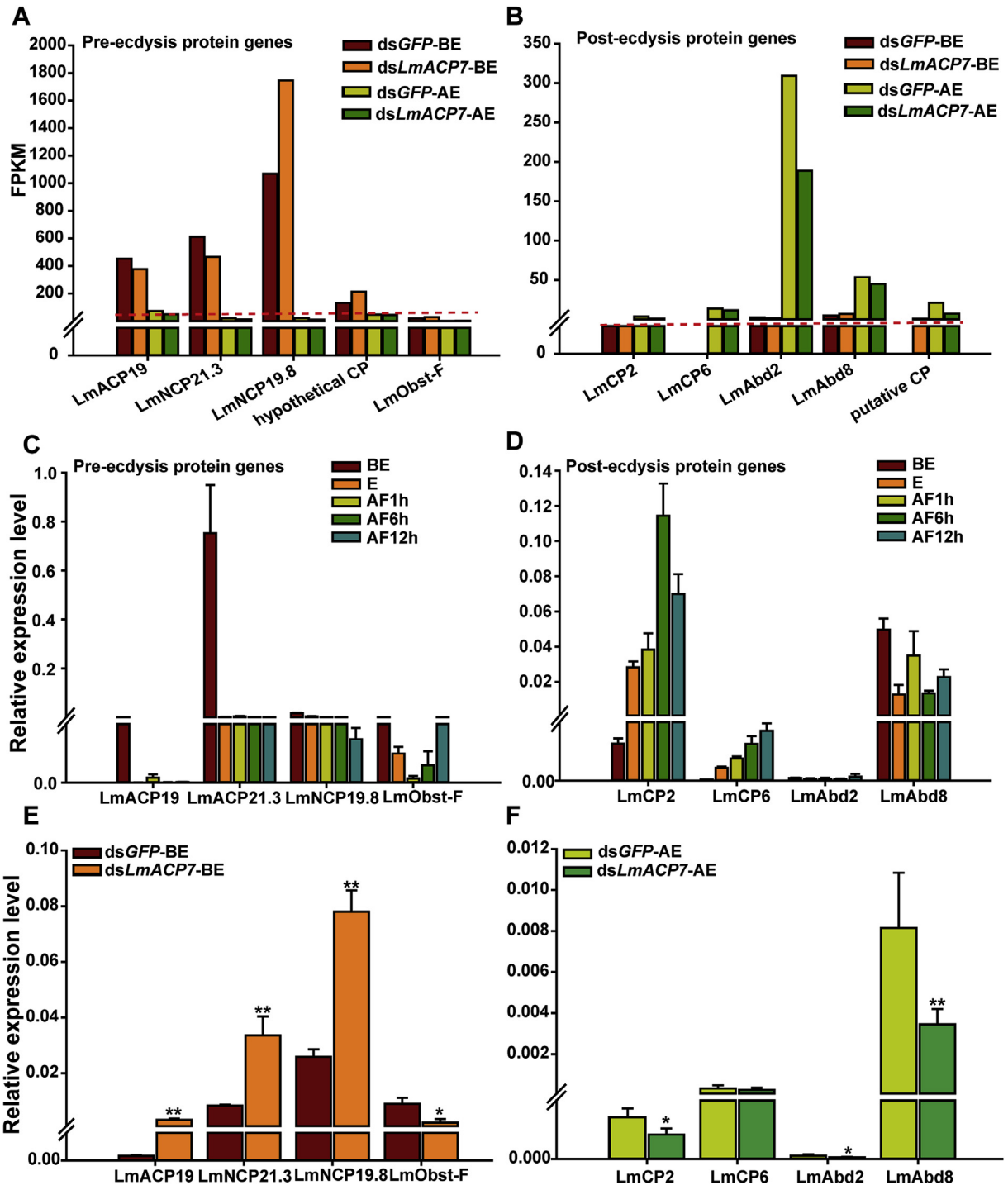

Fig. 7. The expression of exocuticle and endocuticle protein genes during molting of wings, and after deficiency of *LmACP7* by RNAi.
A-B. The expression of post-ecdysis protein coding genes and pre-ecdysis protein coding genes were identified based on the transcriptome data. **C-D.** The expression of post-ecdysis protein coding genes and pre-ecdysis protein coding genes were determined at before ecdysis, at ecdysis, and after ecdysis (1, 6, and 12 h) from nymph to adult transition by RT-qPCR. **E-F.** The expression of post-ecdysis protein coding genes and pre-ecdysis protein coding genes were determined at before ecdysis and after ecdysis injected ds*LmACP7* or ds*GFP* at day 2 of fifth instar nymphs. *RPL32* was used as the reference control. Data are reported as means ± SE of three independent biological replications; asterisks indicate significant differences, *, $P < 0.05$, **, $P < 0.01$. BE: before ecdysis; E: ecdysis; AE: after ecdysis.

4.2. LmACP7 mainly locates in the exocuticle of adult wing cuticle

The insect cuticle is a protective and supportive material covering the entire insect outer body. The main components of cuticle are chitin filaments embedded in a matrix of various proteins. The composition as well as the mechanical properties of the cuticle are regionally specialized, and the various layers of the cuticle may also differ in their composition and properties accordingly. The outer layer of the cuticle is deposited during the pharate period preceding ecdysis (pre-ecdysial cuticle, exocuticle) and the inner layer is deposited after ecdysis (post-ecdysial cuticle, endocuticle). To distinguish from the cuticular proteins deposited during the post-ecdysial period, cuticular proteins deposited during this period are called pre-ecdysial proteins. The pre-ecdysial part of the procuticle is in some regions stabilized by the process of

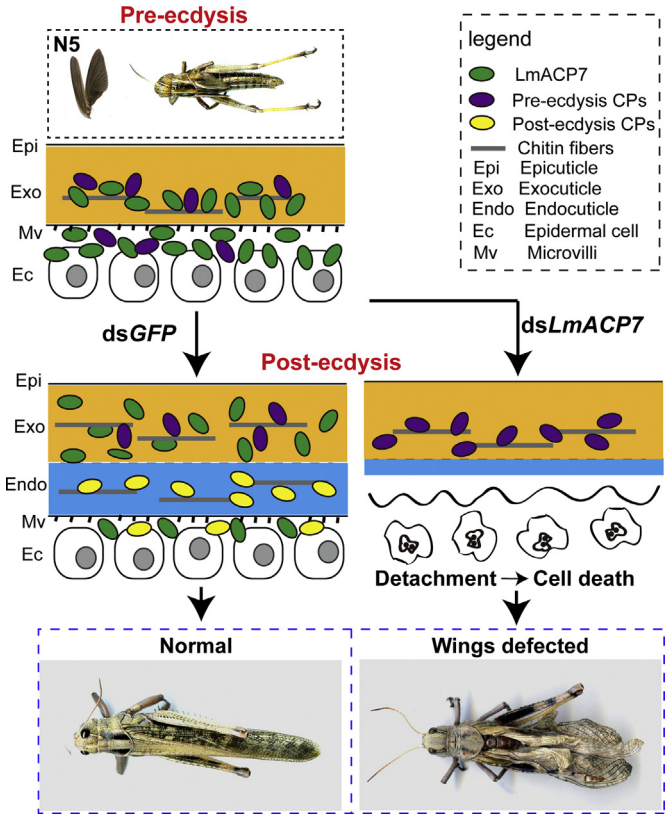

Fig. 8. Model of locust wing metamorphosis mediated by LmACP7
LmACP7 is specifically expressed at the pre-ecdysial stage in locust wings, localizes to the exocuticle and mediates the adhesion of the exocuticle to the apical plasma membrane of wing epithelial cells that continue to produce the endocuticle. Loss of LmACP7 function causes detachment of the cuticle from the epithelial cells and disruption of the microvilli thereby triggering an apoptosis or apoptosis-like response during wing development. Finally, the adult wings fail to elongate fully.

sclerotization, whereby the cuticle is hardened and the proteins are made unextractable, presumably due to cross-linking. In other cuticular regions, the pre-ecdysial proteins remain unmodified, and the cuticle stays soft and flexible. In the present study, we found that LmACP7 was specifically accumulated in the pre-ecdysial procuticle of locust wings (Fig. 2), and was able to bind to chitin *in vitro* (Fig. S6). The precise localization of LmACP7 protein showed that LmACP7 was mainly present in the exocuticle but not in the endocuticle of adult wings (Fig. 3). Based on these data, we conclude that LmACP7 may be involved in the process of sclerotization, probably interacting with other cuticle proteins and chitin. In the beetle *T. castaneum*, interaction between TcCPR27, TcCPR18 and TcCP30, which are the most abundant cuticular proteins in elytra, has been analyzed providing important insight into the roles of CPs in organizing the cuticle and defining its properties (Arakane et al., 2012; Mun et al., 2015; Noh et al., 2014, 2015). Possible cross-linking partners LmACP7 need to be identified and characterized in further studies in order to understand the function of CPs in a flyable wing.

4.3. Reduced LmACP7 function causes a disorder of epithelial cells and promotes apoptosis in locust wings

The insect wings are composed of ventral and dorsal layers of epithelial cells. In the epithelium, cells either lose their adhesiveness and delaminate or undergo apoptosis (Bloor and Kiehart, 2002). In *B. mori.*, a cuticular protein with low complexity sequence, BmorCPH24, was shown to be involved in the synthesis of endocuticle and its disruption induced apoptosis of epidermal cells that was accompanied by reducing expression of R&R-type larval cuticle protein genes (Xiong et al., 2017). Apoptosis (a classical programmed cell death, PCD) plays essential roles in development and diseases (Green, 2005; He and Klionsky, 2009). Apoptosis culminates in cellular shrinkage with nuclear chromatin condensation and nuclear fragmentation, and can be influenced by many extracellular and intracellular signals, including growth factors, DNA-damaging agents, hormones, and nutrients (Ferraro and Cecconi, 2007). However, how a structural protein such as LmACP7 induces cell apoptosis or a similar process remains unclear.

A major finding based on several lines of evidence was that deficiency of LmACP7 causes a disorder of wing epithelial cells and induces apoptosis-like event during locust molting. First, compared to the control situation, the epithelial cells of wings from ds*LmACP7*-injected insects exhibited cell debris, and organelles and cell structures such as the endoplasmic reticulum, mitochondria, the microvilli and cell junctions were degraded (Fig. 5). Additionally, we also found that the lamellae in the region connecting the endocuticle and the apical plasma membranes of wing epithelial cells were disrupted. As reported by Bloor and Kiehart in *D. melanogaster*, cells either lose their adhesiveness and delaminate from the epidermis or undergo apoptosis in the ventral epidermis when cell-cell adhesion is disrupted (Bloor and Kiehart, 2002). Transcripts of genes coding for cell junctions protein (*Nectin*, *Coracle*, *Arm*, *Crumbs*, *Dachsous*, *Dlg-5* and *Dlg-1*) were decreased in the ds*LmACP7*-treated insects after ecdysis. In addition, the *hippo* pathway genes (*Warts*, *Merlin*, *Expanded*, *Hippo*, *Yorkie*) were also reduced in the ds*LmACP7*-treated insects after ecdysis, and these genes have been reported to induce apoptosis (Liu et al., 2016; Yu and Guan, 2013).

Second, compared to the ds*GFP*-treated control insects, nuclear chromatin condensation, pyknosis and karyorrhexis in the ds*LmACP7*-treated insects were observed after ecdysis by TEM, but not before ecdysis (Fig. 5). In addition, after ecdysis, caspase-3 and caspase-9 activities dramatically increased in the ds*LmACP7*-treated insects compared to ds*GFP*-treated control insects (Fig. 6). Additionally, mRNA levels of several important apoptosis genes were up-regulated in the ds*LmACP7*-treated insects after ecdysis (Fig. S8). Together, all these results indicated that deficiency of LmACP7 promotes apoptosis or an apoptosis-like process during locust molting by causing structural abnormalities in the endocuticle secreted by epidermal cells.

Based on these studies, we propose a hypothesis for the roles of LmACP7 during locust wing metamorphosis (Fig. 8). LmACP7 is specifically expressed at the pre-ecdysial stage in locust wings, localizes to the exocuticle and mediates the adhesion of the exocuticle to the apical plasma membrane of wing epithelial cells that continue to produce the endocuticle. Loss of LmACP7 function causes detachment of the cuticle from the epithelial cells and disruption of the microvilli thereby triggering a premature apoptosis or an apoptosis-like response during wing development. Finally, the adult wings fail to elongate fully. These results indicate that the CPR protein, LmACP7 is an essential structural component of the wing cuticle and is required for the integrity of wing epithelial cells during development. Our results not only contribute to better understand the molecular mechanism how a structural protein in the flyable wing cuticle affect wing morphogenesis, but also highlight a new and specific target gene for migratory pests control.

Author contribution

XM. Zhao, X. Gou and JZ. Zhang designed the research; XM. Zhao, X. Gou and WM. Liu performed the research; XM. Zhao, X. Gou, S. Li, EB. Ma and JZ. Zhang analyzed the data; and XM. Zhao, X. Gou, K.Y. Zhu, M. Bernard and JZ. Zhang wrote the paper. All authors reviewed the results and approved the final version of the manuscript.

Conflicts of interest

The authors declare that they have no conflicts of interest with the

contents of this article.

Acknowledgments

This work was supported by National Natural Science Foundation of China (Grant No. 31702067, 31730074, 31640075), The Natural Science Foundation of Shanxi Province, China (201601D021102). We thank Dr. Subbaratnam Muthukrishnan (Department of Biochemistry & Molecular Biophysics, Kansas State University, Manhattan, KS 66506) and Dr. Yoonseong Park (Department of Entomology, Kansas State University, Manhattan, KS66506) for helpful comments during the preparation of this manuscript. We acknowledge Dr. Juanjuan Wang from the Scientific Instrument Center at Shanxi University for her help with LSM 880 confocal laser-scanning microscope measurements.

Appendix A. Supplementary data

Supplementary data to this article can be found online at https://doi.org/10.1016/j.ibmb.2019.103206.

References

Appel, E., Heepe, L., Lin, C.P., Gorb, S.N., 2015. Ultrastructure of dragonfly wing veins: composite structure of fibrous material supplemented by resilin. J. Anat. 227, 561–582.

Apple, R.T., Fristrom, J.W., 1991. 20-Hydroxyecdysone is required for, and negatively regulates, transcription of *Drosophila* pupal cuticle protein genes. Dev. Biol. 146, 569–582.

Arakane, Y., Lomakin, J., Gehrke, S.H., Hiromasa, Y., Tomich, J.M., Muthukrishnan, S., Beeman, R.W., Kramer, K.J., Kanost, M.R., 2012. Formation of rigid, non-flight forewings (elytra) of a beetle requires two major cuticular proteins. PLoS Genet. 8, e1002682.

Bloor, J.W., Kiehart, D.P., 2002. RhoA regulates the cytoskeleton and cell-cell adhesion in the developing epidermis. Development 129, 3173–3183.

Charles, J., Bouhin, H., Quennedey, B., Courrent, A., Delachambre, J., 1992. cDNA cloning and deduced amino acid sequence of a major, glycine-rich cuticular protein from the coleopteran *Tenebrio molitor*. Eur. J. Biochem. 206, 813–819.

Charles, J.P., 2010. The regulation of expression of insect cuticle protein genes. Insect Biochem. Mol. Biol. 40, 205–213.

Chen, J., Dai, G., Xu, Y., 2007. Optimal composite structures in the forewings of beetles. Compos. Struct. 81, 432–437.

Cornman, R.S., Togawa, T., Dunn, W.A., He, N., Emmons, A.C., Willis, J.H., 2008. Annotation and analysis of a large cuticular protein family with the R&R Consensus in *Anopheles gambiae*. BMC Genomics 22, 1–16.

Deng, H., Li, Y., Zhang, J., Liu, L., Feng, Q., 2015. Analysis of expression and chitin-binding activity of the wing disc cuticle protein BmWCP4 in the silkworm, *Bombyx mori*. Insect Sci. 22, 1–9.

Dittmer, N.T., Hiromasa, Y., Tomich, J.M., Lu, N., Beeman, R.W., Kramer, K.J., Kanost, M.R., 2012. Proteomic and transcriptomic analyses of rigid and membranous cuticles and epidermis from the elytra and hindwings of the red flour beetle, *Tribolium castaneum*. J. Proteome Res. 11, 269–278.

Ferraro, E., Cecconi, F., 2007. Autophagic and apoptotic response to stress signals in mammalian cells. Arch. Biochem. Biophys. 462, 210–219.

Futahashi, R., Okamoto, S., Kawasaki, H., Zhong, Y.S., Iwanaga, M., Mita, K., Fujiwara, H., 2008. Genome-wide identification of cuticular protein genes in the silkworm, *Bombyx mori*. Insect Biochem. Mol. Biol. 38, 1138–1146.

Green, D.R., 2005. Apoptotic pathways: ten minutes to dead. Cell 121, 671–674.

Guo, Y., Zhang, J., Yang, M., Yan, L., Zhu, K.Y., Guo, Y., Ma, E., 2012. Comparative analysis of cytochrome P450-like genes from *Locusta migratoria manilensis*: expression profiling and response to insecticide exposure. Insect Sci. 19, 75–85.

He, C., Klionsky, D.J., 2009. Regulation mechanisms and signaling pathways of autophagy. Annu. Rev. Genet. 43, 67–93.

Karouzou, M.V., Spyropoulos, Y., Iconomidou, V.A., Cornman, R.S., Hamodrakas, S.J., Willis, J.H., 2007. *Drosophila* cuticular proteins with the R&R Consensus: annotation and classification with a new tool for discriminating RR-1 and RR-2 sequences. Insect Biochem. Mol. Biol. 37, 754–760.

Klarskov, K., Hojrup, P., Andersen, S.O., Roepstorff, P., 1989. Plasma-desorption mass spectrometry as an aid in protein sequence determination. Biochem. J. 262, 923–930.

Klowden, M.J., 2008. Physiological Systems in Insects, second ed. Academic Press, New York, pp. 1–703.

Krogh, T.N., Skou, L., Roepstorff, P., Andersen, S.O., Hojrup, P., 1995. Primary structure of proteins from the wing cuticle of the migratory locust, *Locusta migratoria*. Insect Biochem. Mol. Biol. 25, 319–329.

Lampe, D.J., Willis, J.H., 1994. Characterization of a cDNA and gene encoding a cuticular protein from rigid cuticles of the giant silkmoth, *Hyalophora cecropia*. Insect Biochem. Mol. Biol. 24, 419–435.

Li, Y.L., Song, H.F., Zhang, X.Y., Li, D.Q., Zhang, T.T., Ma, E.B., Zhang, J.Z., 2016. Heterologous expression and characterization of two chitinase 5 enzymes from the migratory locust *Locusta migratoria*. Insect Sci. 23, 406–416.

Liu, S., Zhang, P., Song, H.S., Qi, H.S., Wei, Z.J., Zhang, G., Zhan, S., Liu, Z., Li, S., 2016. Yorkie facilitates organ growth and metamorphosis in Bombyx. Int. J. Biol. Sci. 12, 917–930.

Liu, W., Xie, Y., Xue, J., Gao, Y., Zhang, Y., Zhang, X., Tan, J., 2009. Histopathological changes of Ceroplastes japonicus infected by *Lecanicillium lecanii*. J. Invertebr. Pathol. 101, 96–105.

Liu, X., Li, F., Li, D., Ma, E., Zhang, W., Zhu, K.Y., Zhang, J., 2013. Molecular and functional analysis of UDP-N-acetylglucosamine pyrophosphorylases from the migratory locust, *Locusta migratoria*. PLoS One 8, e71970.

Moussian, B., 2010. Recent advances in understanding mechanisms of insect cuticle differentiation. Insect Biochem. Mol. Biol. 40, 363–375.

Mun, S., Young Noh, M., Dittmer, N.T., Muthukrishnan, S., Kramer, K.J., Kanost, M.R., Arakane, Y., 2015. Cuticular protein with a low complexity sequence becomes cross-linked during insect cuticle sclerotization and is required for the adult molt. Sci. Rep. 5, 10484.

Noh, M.Y., Kramer, K.J., Muthukrishnan, S., Kanost, M.R., Beeman, R.W., Arakane, Y., 2014. Two major cuticular proteins are required for assembly of horizontal laminae and vertical pore canals in rigid cuticle of *Tribolium castaneum*. Insect Biochem. Mol. Biol. 53, 22–29.

Noh, M.Y., Muthukrishnan, S., Kramer, K.J., Arakane, Y., 2015. *Tribolium castaneum* RR-1 cuticular protein TcCPR4 is required for formation of pore canals in rigid cuticle. PLoS Genet. 11, e1004963.

Noh, M.Y., Muthukrishnan, S., Kramer, K.J., Arakane, Y., 2016. Cuticle formation and pigmentation in beetles. Curr. Opin. Insect Sci. 17, 1–9.

Noh, M.Y., Muthukrishnan, S., Kramer, K.J., Arakane, Y., 2017. Development and ultrastructure of the rigid dorsal and flexible ventral cuticles of the elytron of the red flour beetle, *Tribolium castaneum*. Insect Biochem. Mol. Biol. 91, 21–33.

Rajabi, H., Shafiei, A., Darvizeh, A., Dirks, J.H., Appel, E., Gorb, S.N., 2016. Effect of microstructure on the mechanical and damping behaviour of dragonfly wing veins. Roy. Soc. Open Sci. 3, 160006.

Rebers, J.E., Riddiford, L.M., 1988. Structure and expression of a *Manduca sexta* larval cuticle gene homologous to *Drosophila* cuticle genes. J. Mol. Biol. 203, 411–423.

Rebers, J.E., Willis, J.H., 2001. A conserved domain in arthropod cuticular proteins binds chitin. Insect Biochem. Mol. Biol. 31, 1083–1093.

Roer, R., Abehsera, S., Sagi, A., 2015. Exoskeletons across the pancrustacea: comparative morphology, physiology, Biochemistry and genetics. Integr. Comp. Biol. 55, 771–791.

Shimahara, K., Takiguchi, Y., 1988. Preparation of crustacean chitin. Methods Enzymol. 161, 417–423.

Silvert, D., Doctor, J., Quesada, L., Fristrom, J., 1984. Pupal and larval cuticle proteins of *Drosophila melanogaster*. Biochemistry 23, 5767–5774.

Simpson, S.J., Douglas, A.E., 2013. The Insects : Structure and Function/R. F. Chapman, fifth ed. Cambridge University Press.

Togawa, T., Augustine Dunn, W., Emmons, A.C., Willis, J.H., 2007. CPF and CPFL, two related gene families encoding cuticular proteins of *Anopheles gambiae* and other insects. Insect Biochem. Mol. Biol. 37, 675–688.

Togawa, T., Nakato, H., Izumi, S., 2004. Analysis of the chitin recognition mechanism of cuticle proteins from the soft cuticle of the silkworm, *Bombyx mori*. Insect Biochem. Mol. Biol. 34, 1059–1067.

Toprak, U., Baldwin, D., Erlandson, M., Gillott, C., Hegedus, D.D., 2010. Insect intestinal mucins and serine proteases associated with the peritrophic matrix from feeding, starved and moulting *Mamestra configurata* larvae. Insect Mol. Biol. 19, 163–175.

Vannini, L., Willis, J.H., 2017. Localization of RR-1 and RR-2 cuticular proteins within the cuticle of *Anopheles gambiae*. Arthropod Struct. Dev. 46, 13–29.

Willis, J.H., 2010. Structural cuticular proteins from arthropods: annotation, nomenclature, and sequence characteristics in the genomics era. Insect Biochem. Mol. Biol. 40, 189–204.

Xiong, G., Tong, X., Gai, T., Li, C., Qiao, L., Monteiro, A., Hu, H., Han, M., Ding, X., Wu, S., Xiang, Z., Lu, C., Dai, F., 2017. Body shape and coloration of silkworm larvae are influenced by a novel cuticular protein. Genetics 207, 1053–1066.

Yu, F.X., Guan, K.L., 2013. The Hippo pathway: regulators and regulations. Genes Dev. 27, 355–371.

Yu, R., Liu, W., Li, D., Zhao, X., Ding, G., Zhang, M., Ma, E., Zhu, K.Y., Li, S., Moussian, B., Zhang, J., 2016. Helicoidal organization of chitin in the cuticle of the migratory locust requires the function of the chitin deacetylase 2 enzyme (LmCDA2). J. Biol. Chem. 291, 24352–24363.

Zhao, X.M., Liu, C., Li, Q.Y., Hu, W.-B., Zhou, M.T., Nie, H.Y., Zhang, Y.X., Peng, Z.C., Zhao, P., Xia, Q.Y., 2014. Basic helix-loop-helix transcription factor bmsage is involved in regulation of fibroin H-chain gene via interaction with SGF1 in *Bombyx mori*. PLoS One 9, e94091.

Zhao, X., Gou, X., Qin, Z., Li, D., Wang, Y., Ma, E., Li, S., Zhang, J., 2017. Identification and expression of cuticular protein genes based on *Locusta migratoria* transcriptome. Sci. Rep. 7, 45462.

Zhao, X., Qin, Z., Liu, W., Liu, X., Moussian, B., Ma, E., Li, S., Zhang, J., 2018. Nuclear receptor HR3 controls locust molt by regulating chitin synthesis and degradation genes of *Locusta migratoria*. Insect Biochem. Mol. Biol. 92, 1–11.